Influence of thermal effects on buoyancy-driven convection around autocatalytic chemical fronts propagating horizontally

L. Rongy*,[1], G. Schuszter*,[2], Z. Sinkó[2], T. Tóth[2], D. Horváth[2], A. Tóth[2], and A. De Wit[1]

[1] *Nonlinear Physical Chemistry Unit, CP 231, Faculté des Sciences, Université Libre de Bruxelles (ULB), 1050 Brussels, Belgium*

[2] *Department of Physical Chemistry, University of Szeged, Rerrich Béla tér 1., Szeged, H-6720, Hungary*

* *These two persons contributed equally to the work.*

(Dated: March 22, 2009)

Abstract

The spatio-temporal dynamics of vertical autocatalytic fronts traveling horizontally in thin solution layers closed to the air can be influenced by buoyancy-driven convection induced by density gradients across the front. We perform here a combined experimental and theoretical study of the competition between solutal and thermal effects on such convection. Experimentally, we focus on the antagonistic chlorite-tetrathionate reaction for which solutal and thermal contributions to the density jump across the front have opposite signs. We show that in isothermal conditions the heavier products sink below the lighter reactants providing an asymptotic constant finger shape deformation of the front by convection. When thermal effects are present the hotter products, on the contrary, climb above the reactants for strongly exothermic conditions. These various observations as well as the influence of the relative weight of solutal and thermal effects and of the thickness of the solution layer on the dynamics are discussed in terms of a 2D reaction-diffusion-convection model parameterized by a solutal R_C and a thermal R_T Rayleigh number.

I. INTRODUCTION

When two miscible non reactive fluids having different densities are brought to contact in a horizontal solution layer with the interface parallel to the gravity field, the system is always unstable giving rise to a "gravity current" such that the denser solution sinks below the other one until the reach of a stratification of lighter fluid on top of the heavier one[1,2]. Ultimately, the two miscible fluids mix completely to yield one homogeneous solution, the density of which is the average of the densities of each initial separated solution. The situation is drastically different when the density jump acts across a self-organized reactive interface such as a traveling autocatalytic chemical front resulting from the coupling between chemical reactions and diffusion and separating the reactants of density ρ_r from the products of density ρ_p[3–6]. The front experiences a density difference $\Delta\rho = \rho_p - \rho_r = \Delta\rho_S + \Delta\rho_T$ due to a solutal part $\Delta\rho_S$ induced by compositional changes and a thermal part $\Delta\rho_T$ related to the exothermicity of the reaction. For aqueous solutions $\Delta\rho_T$ is always negative above 4 °C as the products are hotter in exothermic reactions, while $\Delta\rho_S$ can have either positive or negative sign depending on whether the products are respectively solute heavier or lighter than the reactants.

Buoyancy-driven instabilities resulting from these density differences across an autocatalytic front have been thoroughly studied in vertical geometries where the front travels along the gravity field[4–12]. In that case, the combination of solutal and thermal contributions to the density jump has been shown to lead to various instability scenarios depending on whether $\Delta\rho_S$ and $\Delta\rho_T$ have the same negative sign (cooperative case) or different signs ($\Delta\rho_S > 0$, $\Delta\rho_T < 0$, antagonistic case)[6,13,14].

In thin horizontal solution layers, it is known that convection can also deform the dynamic of autocatalytic fronts or waves[4,15–21]. In the case of a simple reaction front propagating horizontally, it has been shown both experimentally[17,18,22] and numerically[16,23] that instead of a gravity current leading to a homogeneous solution, the coupling between reaction, diffusion and convection triggered by the density difference leads in isothermal conditions to one solitary vortex structure deforming the front and speeding it up. The vortex rotates clockwise if the products are lighter than the reactants and climb above them ($\Delta\rho_S < 0$)[16,20,23]. On the contrary, the vortex rotates counterclockwise if the products are heavier and sink below the reactants ($\Delta\rho_S > 0$). The situation with positive $\Delta\rho_S$ is symmetric to

the one for negative solutal density jump[23].

If thermal effects come into play, the combination of solutal and thermal density changes can lead to new dynamics for propagation of autocatalytic fronts in horizontal set-ups[24]. It has been shown numerically[25] that, in the cooperative case, the fact that heat diffuses faster than mass can lead to local hot spots behind the front corresponding to a local stratification of heavy fluid on top of a light one. In the antagonistic case, the competition between solutal effects and thermal effects warming up the solute heavy products can give rise to an oscillatory dynamics which is not stationary in a framework moving at the reaction-diffusion-convection speed.

In this context, it is the objective of this article to investigate both experimentally and numerically the influence of antagonistic solutal and thermal effects on the dynamics of exothermic vertical fronts of the chlorite-tetrathionate (CT) reaction[26,27] traveling horizontally in thin covered solution layers. The CT reaction is known to be an exothermic antagonistic autocatalytic reaction with negative $\Delta\rho_T$ but positive $\Delta\rho_S$[11], i.e., the products are solute heavier but hotter than the solute lighter reactants at room temperature. Experimentally, the solutal and thermal effects can be varied independently by modifying the thickness of the reactor and working at different mean temperature. We show then experimentally that in isothermal conditions, the heavy products sink under the lighter reactants while, when heat effects are dominating, the products are sufficiently hot to be lighter and rise above the reactants. The experimental dynamics is discussed in the light of a 2D model coupling the Stokes equation for the flow speed to reaction-diffusion-convection (RDC) equations for the concentration of the autocatalytic product and temperature. Combined experimental and numerical parameter studies allow to analyze the respective role of solutal and thermal effects in the dynamics as well as the influence of the height of the solution layer on the number of rolls observed in concentration fields.

The article is organized as follows: in section I, we describe the experimental results showing the influence of thermal effects on the propagation of fronts. Section II discusses the 2D model and numerical simulations used to understand the competition between solutal and thermal effects while conclusions are drawn in section III.

TABLE I: Composition of reactant solution

$[K_2S_4O_6]$/mM	5
$[NaClO_2]$/mM	20
[NaOH]/mM	2.5
[Congo red]/mM	0.574

II. EXPERIMENTAL

Throughout the experiments reagent-grade chemicals of the CT reaction were used (Sigma, Aldrich, Reanal) with the exception of sodium-chlorite, which was recrystallized twice from the commercially available technical-grade material.[28] A Hele-Shaw cell was constructed with two 8 mm thick Plexiglas walls of length $L_x = 50$ cm with a gap width of height L_z set to 1, 1.5, 2, 2.5, 3, or 4 cm and a thickness L_y equal to 1, 2, or 3 mm (see Fig.1). Once the cell was filled with the reactant solution with composition in Table 1, two vertically oriented Pt wires (0.25 mm in diameter) served as front initiator by applying a 3 V potential difference between them for a few seconds. The horizontally propagating reaction fronts were monitored by a CCD camera attached to a computer-driven imaging system, which captured the images at 2–10 s intervals. The acidity fronts were visualized by congo red pH indicator, while enhanced contrast was achieved by an appropriate cut-off filter. For experiments at 3 °C the solution was previously cooled, then poured in the Hele-Shaw cell sandwiched between two thermostated transparent jackets. Fronts were initiated once the system reached the required temperature. The solution densities at both 3 °C and room temperatures were measured by an AP Paar DMA 58 digital densitometer within 10^{-5} g/cm^3 precision.

The front position was given as the point of inflection in the gray scale values along the direction of propagation (x coordinate), from which the mean front position was determined by averaging it along the direction perpendicular to propagation (z coordinate). For stable patterns the final front geometry was characterized by the mixing length and the temporal average of the front profiles. The mixing length was defined as the standard deviation of the mean front position, while the temporal average was the time average of the front profiles with the mean front position shifted to zero.

Under isothermal conditions the products of the CT reaction system are denser than the

reactants and the system exhibits simple convection[11]. In an experimental setup this condition may be obtained by using small reactant concentrations in a very thin solution layer, in which case the heat evolved is effectively dissipated to the surrounding. A horizontally propagating vertical chemical front therefore yields a gravity current in which the heavier products sink under the fresh lighter reactants.[22] For an exothermic reaction in thicker solutions the thermal contribution that would otherwise result in multicomponent convection may be best eliminated by running the reaction in aqueous solution at 3 °C, where an anticipated 1–2 °C increase in temperature only leads to negligible thermal contribution to the density change.

The simple convection due to such a solutal density jump leads hence to a deformed front propagating at constant velocity and with constant shape after a short transition period. By increasing the thickness of the solution layer, the convective motion is enhanced as the fluid velocity in the bulk increases leading to longer mixing lengths as shown in Fig.2(a-c).

The mixing length scales with the height in Fig.2 according to

$$L_m/L_0 \;=\; (0.56 \pm 0.03)\; (L_z/L_0)^{1.19\pm0.04} \text{ for } L_y = 1 \text{ mm}, \tag{1}$$

$$L_m/L_0 \;=\; (0.95 \pm 0.10)\; (L_z/L_0)^{1.34\pm0.09} \text{ for } L_y = 2 \text{ mm}, \tag{2}$$

$$L_m/L_0 \;=\; (1.32 \pm 0.13)\; (L_z/L_0)^{1.31\pm0.08} \text{ for } L_y = 3 \text{ mm} \tag{3}$$

with $L_0 = 1$ cm unit length. The coefficients of the scaling laws increase with height as anticipated, while the exponent can be considered as constant (1.31 ± 0.09) because the change in it is within the experimental error as shown below.

At room temperature, on the contrary, the thermal density jump across the front plays an important role. The heat evolution in the course of the reaction leads indeed to a smaller total increase in the density, resulting in mixing lengths shorter than those observed for the appropriate width at 3 °C as presented in Fig.2(d,e). For a solution thickness of 3 mm, a different scenario occurs. Due to the ineffective heat loss to the surrounding, the thermal contribution now dominates, therefore the warmer products are less dense than the fresh reactants across the front. The gravity current is inverted and the warm products accumulate above the reactants. A constant front profile does not exist as previously because the products start to cool and hence sink following the autocatalytic reaction, resulting in a row of convection rolls as seen in Fig.2(f).

The number of cellular deformations trailing the leading tip of the front on the top

boundary increases with the height of the solution layer as their intrinsic size is observed to be generally independent of the height (see Fig.4).

III. THEORETICAL ANALYSIS

In experiments, the geometry is effectively three dimensional. Solutal effects are varied when varying the thickness L_y which changes the relative importance of friction forces on the wall. In parallel, thermal effects can be either eliminated by performing the experiments at 3°C or varied by performing the experiment at room temperature but increasing the thickness L_y. This decreases the relative importance of heat losses in the dynamics and effectively increases the temperature of the products. Fortunately, a 2D model is found to capture the important qualitative features of the system. Indeed in practice, the dynamics results from the competition between solutal and thermal effects the relative importance of which can be casted into Rayleigh numbers of a 2D model as we show it now.

A. Model

To gain insight into the influence of competing solutal and thermal effects on the dynamics of fronts, we turn to numerical simulations of a simple 2D dimensionless model[23] coupling the Stokes equation (4) for the 2D velocity $\underline{v} = (u, w)$ of the flow to RDC equations for the concentration c of the autocatalytic product involved into a cubic kinetics (6) and for the temperature T (7). The dimensionless governing equations read

$$\underline{\nabla} p = \nabla^2 \underline{v} + (R_C\, c + R_T\, T)\, \underline{i}_z \,, \tag{4}$$

$$\underline{\nabla} \cdot \underline{v} = 0 \,, \tag{5}$$

$$\frac{\partial c}{\partial t} + \underline{v}.\underline{\nabla} c = \nabla^2 c + c^2(1-c) \,, \tag{6}$$

$$\frac{\partial T}{\partial t} + \underline{v}.\underline{\nabla} T = Le \nabla^2 T + c^2(1-c) \,, \tag{7}$$

where $\underline{i}_z$ is the unit vector in the z-direction, p is the pressure and the Lewis number, $Le = D_T/D$, is the ratio between the thermal D_T and molecular D diffusivities. The dimensionless solutal and thermal Rayleigh numbers, R_C and R_T, are defined respectively

as

$$R_C = -\frac{\partial \rho}{\partial c}\frac{a_0\, L_c^3\, g}{D\,\mu}\,, \tag{8}$$

$$R_T = -\frac{\partial \rho}{\partial T}\frac{\Delta T\, L_c^3\, g}{D\,\mu}\,, \tag{9}$$

where $\partial\rho/\partial c$ and $\partial\rho/\partial T$ are the solutal and thermal expansion coefficients of the solution, respectively. L_c is a characteristic reaction-diffusion length scale[23], a_o the initial concentration of the reactant, g the gravitational acceleration and μ the viscosity of the solution. The solutal Rayleigh number R_C is positive if the density decreases in the course of reaction and negative otherwise while the thermal Rayleigh number R_T is always positive since the reaction is exothermic ($\Delta T > 0$) and $\partial\rho/\partial T$ is negative for water at $T > 4$ °C. For experiments performed at 3 °C, we have $\partial\rho/\partial T \sim 0$ and hence $R_T \sim 0$ effectively, i.e., we explore an isothermal situation. The dimensionless density field is explicitly obtained as

$$\rho(x,z,t) = -R_C\, c(x,z,t) - R_T\, T(x,z,t)\,. \tag{10}$$

Ahead of the front, the reactants (where $c = T = 0$) have a dimensionless density $\rho_r = 0$ due to our choice of non-dimensionalization, while the dimensionless density of the products behind the front (where $c = T = 1$) is $\rho_p = -R_C - R_T$.

Numerical solutions of equations (4-7) are analyzed on a 2D domain of height L_z and width L_x using the numerical procedure described in Ref.[23]. At each boundary of the domain we require zero-flux boundary conditions for the chemical concentration c and the temperature T. The hydrodynamic boundary conditions are rigid walls with no slip for the vertical boundaries and slip walls for the horizontal boundaries, i.e.,

$$\frac{\partial c}{\partial x} = \frac{\partial T}{\partial x} = u = \frac{\partial w}{\partial x} = 0 \qquad \text{at } x = 0\,,\ x = L_x\,, \tag{11}$$

$$\frac{\partial c}{\partial z} = \frac{\partial T}{\partial z} = u = w = 0 \qquad \text{at } z = 0\,,\ z = L_z\,, \tag{12}$$

where L_x and L_z now represent the dimensionless length and height of the layer, respectively. The length of the system and slip walls do not influence the results as long as the reactor length is taken sufficiently long for the front not to interact with a lateral boundary on the time of interest.

B. Results

In experiments performed at 3 °C where thermal effects can be neglected, the length of the finger is larger when the thickness L_y of the cell increases. This effect cannot be captured by the present 2D model other than by understanding that increasing L_y decreases friction effects which could be understood as working with a larger effective R_C. A numerical study of the influence of increasing R_C shows that this leads to longer fingers[23] in agreement with the experimental results of Fig.2(a-c). Increasing the height L_z in isothermal conditions leads to a change of the numerical mixing length as $0.692L_z^2$ which in dimensional units gives for the cubic scheme used here $L_m = 0.692\ a_o\sqrt{(k/D)}L_z^2$, where k denotes a kinetic constant. The equation illustrates that a scaling law exists with an exponent greater than the one observed experimentally. The value itself, however, is different (see (1)-(3)) therefore for quantitative comparison, a full 3D modeling is necessary.

The relative effects of solutal and thermal density changes across the front can however well be captured by fixing R_C to a given negative value such that the products are solute heavier than the reactants and varying R_T. Increasing R_T from zero corresponding to an isothermal situation up to larger positive values describes the expected situation for fronts with increasing exothermicity (see Fig.5). We fix therefore $R_C = -10$ and first start from $R_T = 0$ to have a pure solutal effect like the one studied at 3 °C. There the products are heavier and sink below the reactants as seen on both experimental (Fig.2(a-c)) and numerical (Fig.5top) results. Then we increase R_T, so the products progressively become hotter and thus lighter. First the thermal effect is weak (see $R_T = +5$ in Fig.5), hence it is only slightly stabilizing the solutal effects but does not revert the sinking of the products. For $R_T = 10$, the total density jump across the front is zero but nevertheless we see convection because heat and mass do not diffuse at the same rate ($Le \neq 1$) which leads to an uneven distribution of density. For $R_T = 15$ we obtain an oscillatory regime previously described in details[25]. At larger R_T, the front reverses its deformation with products being now sufficiently hotter and hence sufficiently lighter to climb on top of the reactants at room temperature just as seen experimentally when heat effects are increased when comparing Fig.2(d-e) with Fig.2(f).

When thermal effects are sufficiently strong to lead to rising products, the intensity of the front deformation is observed experimentally to increase with the cell height L_z (Fig.4). To understand this effect, we have numerically investigated the effect of increasing L_z keeping

the Rayleigh numbers to the values $R_C = -10, R_T = +15$ allowing to obtain rising products. We see on Fig.6 that the concentration field becomes more and more distorted when L_z increases. For $L_z = 10$ we observe only one oscillatory tongue deforming periodically the concentration field while an increasing number of tongues is obtained for larger L_z. A close inspection of the related stream function field shown in Fig.7 reveals that increasing L_z does not increase the number of vortices which remains here equal to 3 but rather their lateral extension and intensity. The concentration field inside the finger is therefore increasingly distorted and shows more and more recirculating zones as seen both experimentally (Fig.4) and numerically (Fig.6) even though the underlying velocity field keeps the same number of vortices. Further work to compare the concentration field measured by color changes like on Fig.4 with particle image velocimetry measurements in absence of any color indicator of the reaction would be interesting as it may give insight into the details of the underlying velocity field.

IV. CONCLUSIONS

The competition between solutal and thermal contributions to a density jump across an antagonistic autocatalytic chemical front can lead to different spatio-temporal dynamics depending on the relative weight of each effect. We have investigated here such various situations both experimentally and numerically. In experiments performed with the antagonistic CT system, isothermal conditions are obtained by performing experiments at 3 °C while increasing thermal effects are achieved by increasing the thickness of the reactor to decrease the influence of thermal losses. In a 2D model of the system, the relative importance of each effect can be modulated by varying the relative values of the solutal R_C and thermal R_T Rayleigh numbers. In pure isothermal conditions, the solute heavier products sink below the reactants while if heat effects are important enough to heat the products and make them globally lighter than the reactants, a finger with reversed shape, i.e., hot products rising on top of the colder reactants is obtained. It is found both experimentally and numerically that the spatio-temporal dynamics and the number of cellular deformations observed in the concentration field increase with the magnitude of thermal effects.

Acknowledgments

L.R. is supported by a FNRS (Belgium) PhD fellowship. A.D. acknowledges financial support from Prodex (Belgium), FNRS and from the "Communauté française de Belgique" (Archimedes program). Á.T. is grateful for the financial support from the Hungarian Scientific Research Fund (K72365) and from ESA (PECS 98036). Our collaboration has benefited from support of ESA and from a Hungarian-Belgian NKTH-CGRI agreement.

References

[1] J.E.Simpson, Gravity Current in the Environment and in the Laboratory, (Cambridge University press, 2nd edition, 1997).

[2] C. Härtel, E. Meiburg, and F. Necker, J. Fluid Mech. **418**, 189 (2000).

[3] I.R. Epstein and J.A. Pojman, An Introduction to Nonlinear Dynamics: Oscillations, Waves, Patterns, and Chaos, Oxford University Press, Oxford, 1998.

[4] I. Nagypál, Gy. Bazsa and I.R. Epstein, J. Am. Chem. Soc. **108**, 3635 (1986) .

[5] J.A. Pojman and I.R. Epstein, J. Phys. Chem. **94**, 4966 (1990).

[6] J.A. Pojman, I.R. Epstein, T.J. McManus, and K. Showalter, J. Phys. Chem. **95**, 1299 (1991).

[7] D.A. Vasquez, J.W. Wilder and B.F. Edwards, J. Chem. Phys. **98**, 2138 (1993).

[8] M.R. Carey, S.W. Morris, P. Kolodner, Phys. Rev. E **53**, 6012-6015 (1996).

[9] M. Böckmann and S. C. Müller, Phys. Rev. Lett. **85**, 2506 (2000).

[10] A. De Wit, Phys. Rev. Lett. **87**, 054502 (2001).

[11] D. Horváth, T. Bánsági Jr, and Á. Tóth, J. Chem. Phys. **117**, 4399 (2002).

[12] J. Yang, A. D'Onofrio, S. Kalliadasis and A. De Wit, J. Chem. Phys. **117**, 9395 (2002).

[13] T. Tóth, D. Horváth, and Á. Tóth, Chem. Phys. Lett. **442**, 289?292 (2007).

[14] J. D'Hernoncourt, A. Zebib, and A. De Wit, Chaos **17**, 013109 (2007).

[15] T. Plesser, H. Wilke, and K.H. Winters, Chem. Phys. Lett. **200**, 158 (1992).

[16] D.A. Vasquez, J.M. Littley, J.W. Wilder, and B.F. Edwards, Phys. Rev. E **50**, 280 (1994).

[17] I.P. Nagy, A. Keresztessy, J.A. Pojman, G. Bazsa and Z. Noszticzius, J. Phys. Chem. **98**, 6030 (1994).

[18] A. Keresztessy, I.P. Nagy, G. Bazsa and J.A. Pojman, J. Phys. Chem. **99**, 5379 (1995).

[19] H. Wilke, Physica D **86**, 508 (1995).

[20] Y. Wu, D.A. Vasquez, B.F. Edwards and J.W. Wilder, Phys. Rev. E **51**, 1119 (1995).

[21] M.A. Budroni, M.Masia, M. Rustici, N. Marchettini and V.,Volpert, J. Chem. Phys. **130**, 024902 (2009).

[22] G. Schuszter, T. Tóth, D. Horváth, and Á. Tóth, Phys. Rev. E, **79**, 016216 (2009).

[23] L. Rongy, N. Goyal, E. Meiburg, and A. De Wit, J. Chem. Phys. **127**, 114710 (2007).

[24] M. Belk, K.G. Kostarev, V. Volpert and T.M. Yudina, J. Phys. Chem B **107**, 10292 (2003).

[25] L. Rongy and A. De Wit, submitted to J. Chem. Phys.

[26] L. Szirovicza, I. Nagypál, and E. Boga, J. Amer. Chem. Soc. **111**, 2842 (1989).

[27] D. Horváth and Á. Tóth, J. Chem. Phys. **108**, 4 (1998).

[28] Á. Tóth, D. Horváth and A. Siska, J. Chem. Soc., Faraday Trans. **93**, 73 (1997).

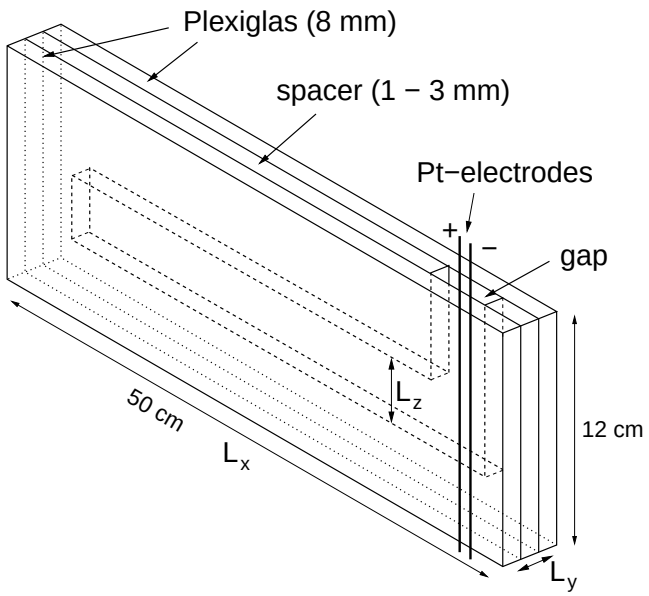

FIG. 1: Sketch of the experimental set-up. The gap in which the front propagates has a length L_x, a height L_z, and a thickness L_y.

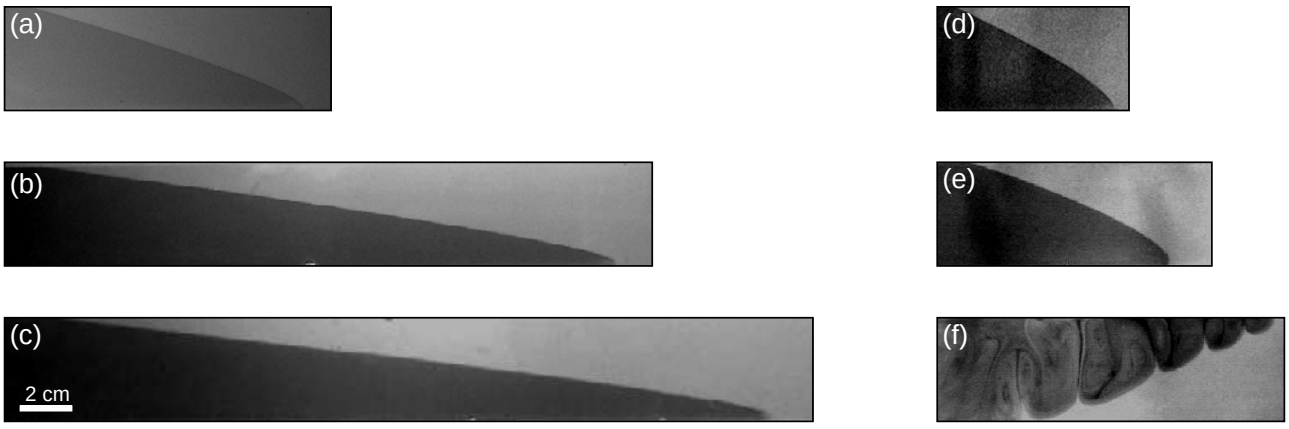

FIG. 2: Comparison of experimental dynamics without (a-c) and with (d-f) heat effects in a system of thickness L_y =1 mm, 2 mm and 3 mm from top to bottom with $L_z = 4$ cm.

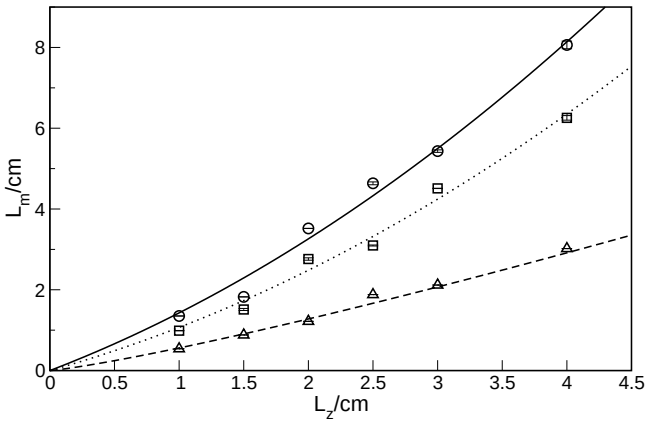

FIG. 3: Dimensional experimental mixing length L_m of the front deformation as a function of the height L_z of the layer for three different thicknesses L_y: 1 mm (△); 2 mm (□); 3 mm (◯) for experiments performed at 3 °C, i.e., for the fingers shown on Fig.2 (a-c), in turn.

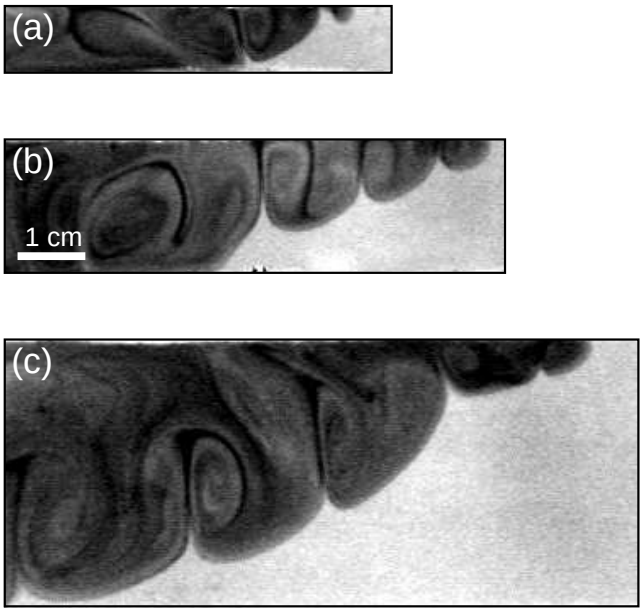

FIG. 4: Influence of the height of the layer L_z on the number of rolls observed experimentally in the concentration field when solutal and thermal effects are competing. From top to bottom L_z = 1 cm (a), 2 cm (b) and 4 cm (c), in turn in a system with thickness $L_y = 3$mm.

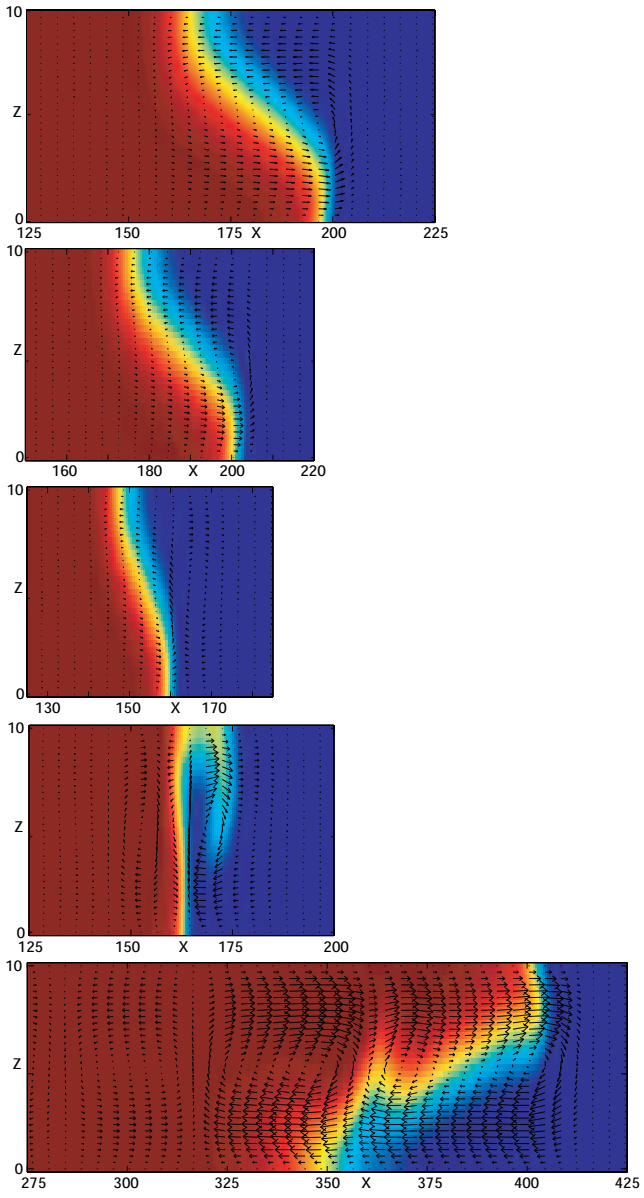

FIG. 5: Numerical study of the influence of increasing thermal effects for a fixed dimensionless layer thickness $L_z = 10$ with $Le = 5$, $R_C = -10$, and $R_T = 0$; 5; 10; 15; 50 from top to bottom. The z direction has been magnified in order to see the details of the velocity field, but the five panels are displayed at the same scale.

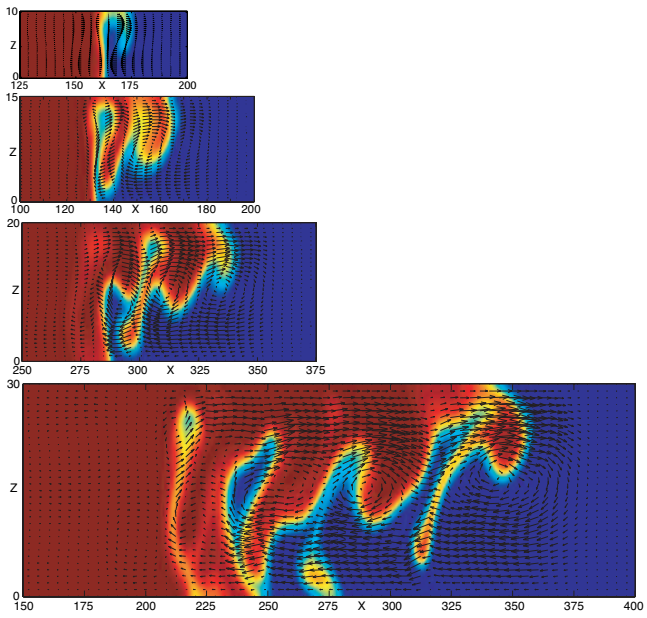

FIG. 6: Numerical study of the influence of the dimensionless height of the layer L_z observed when solutal and thermal effects are competing with $Le = 5,\ R_C = -10,\ R_T = 15$ and $L_z = 10; 15; 20; 30$ from top to bottom. The z direction has been magnified in order to see the details of the velocity field, but the four panels are displayed at the same scale.

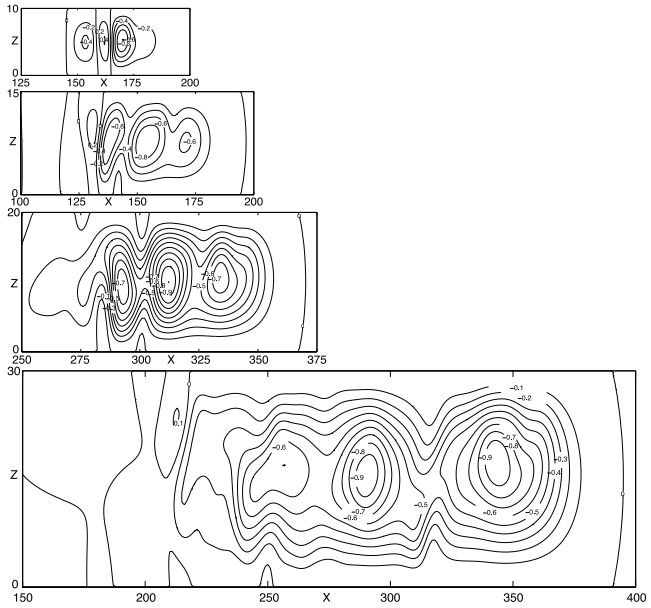

FIG. 7: Numerical study of the influence of the dimensionless height of the layer L_z on the intensity of vortices seen in the stream function plots with $Le = 5$, $R_C = -10$, $R_T = 15$ and $L_z = 10; 15; 20; 30$ from top to bottom. The stream function is renormalized between 0 and 1 and is plotted at the same scale as in Fig.6.

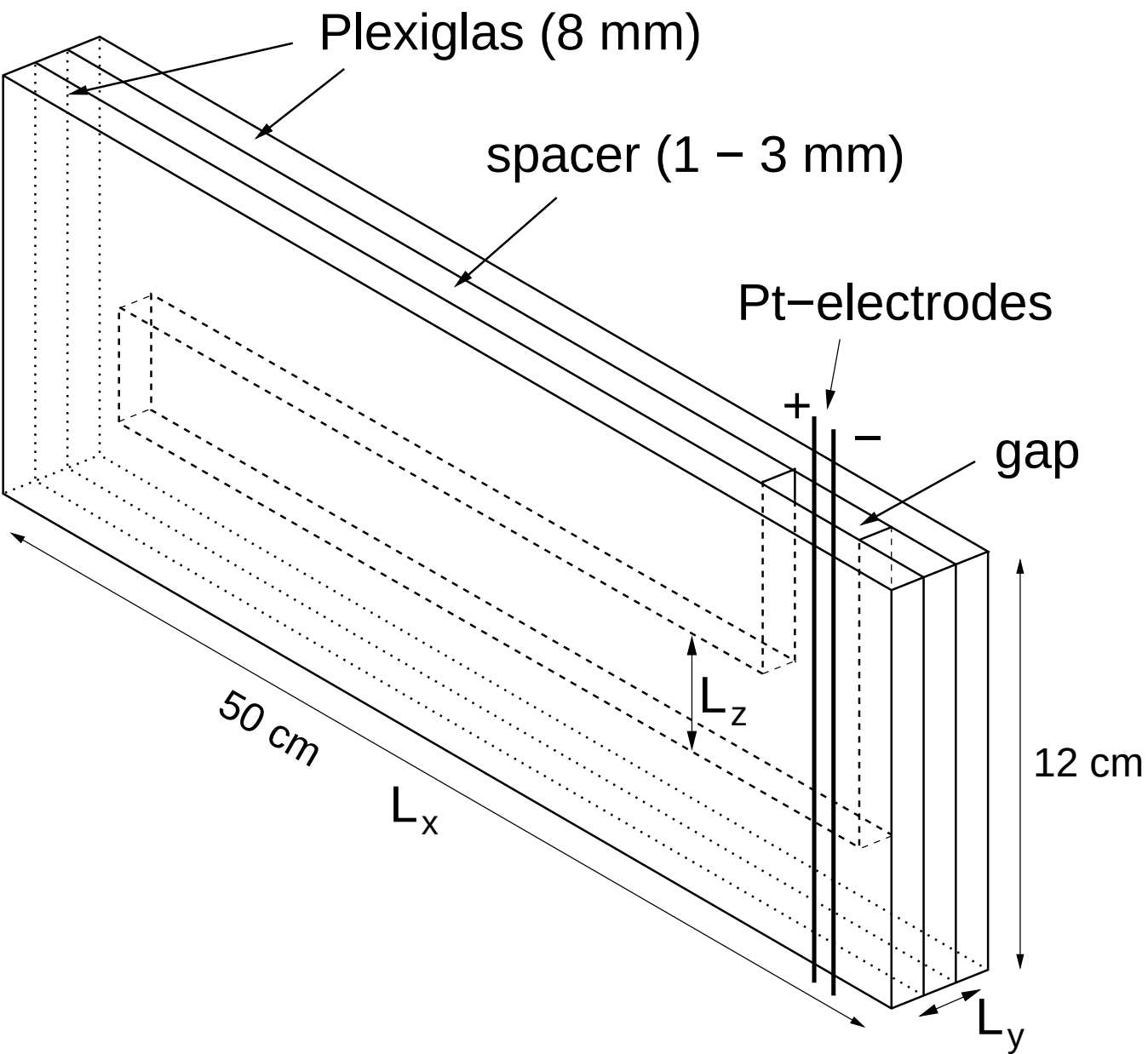
Plexiglas (8 mm)
spacer (1 − 3 mm)
Pt−electrodes
+
−
gap
L_z
50 cm
L_x
12 cm
L_y

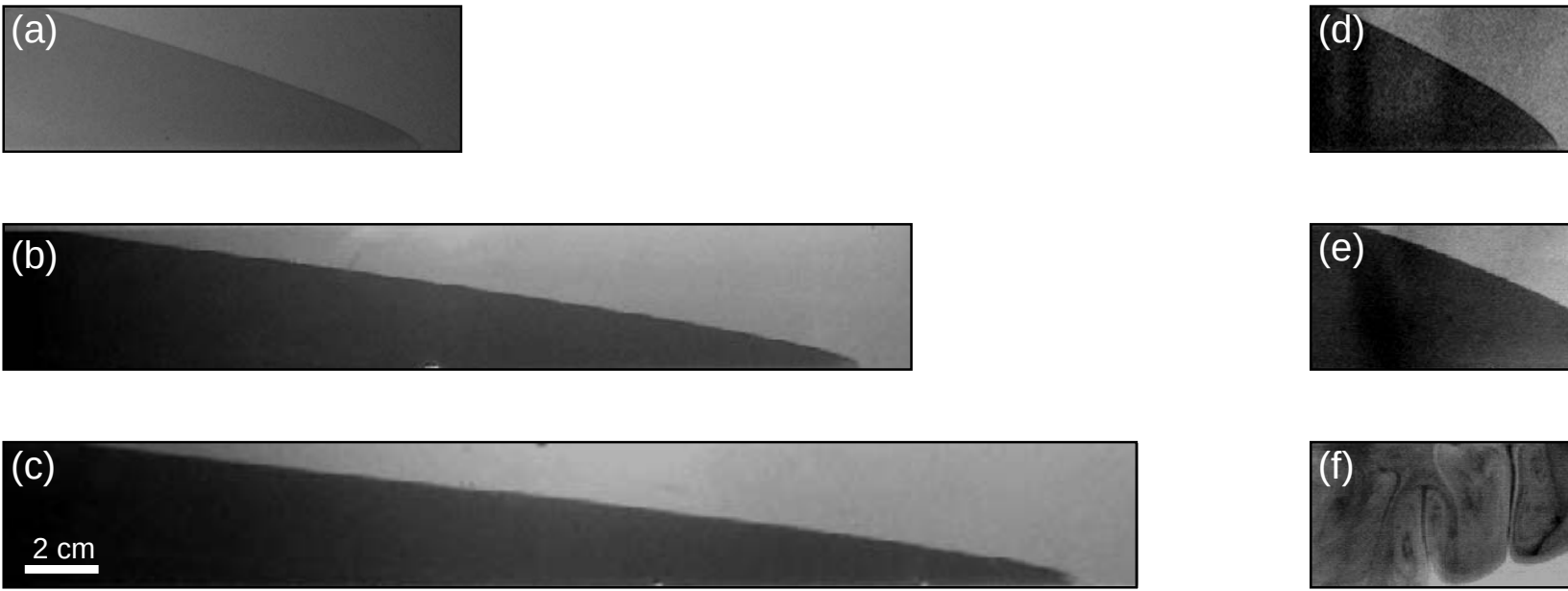
(a)
(b)
(c)
2 cm
(d)
(e)
(f)

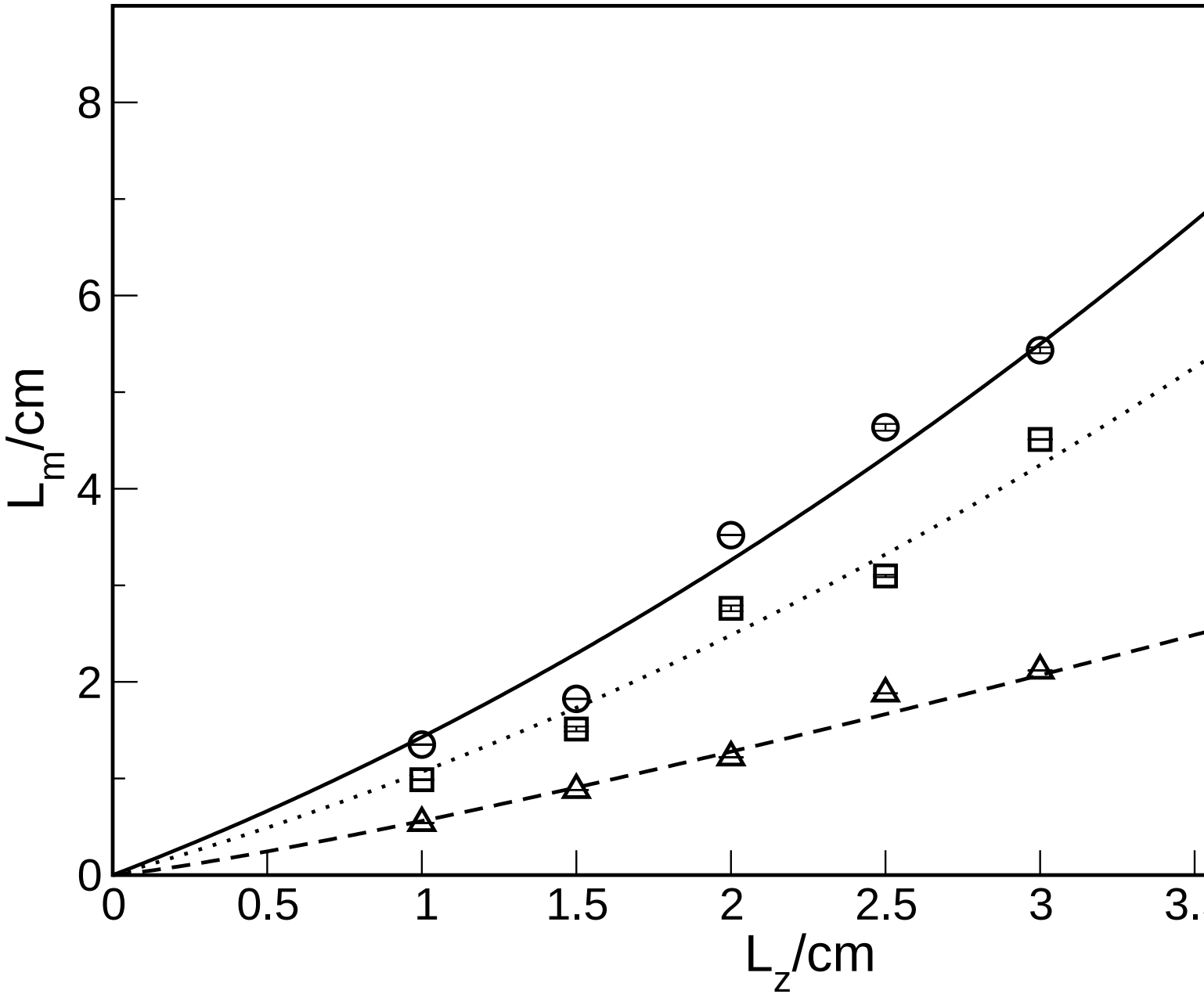
8
6
4
2
0
L_m/cm
0
0.5
1
1.5
2
2.5
3
3.
L_z/cm

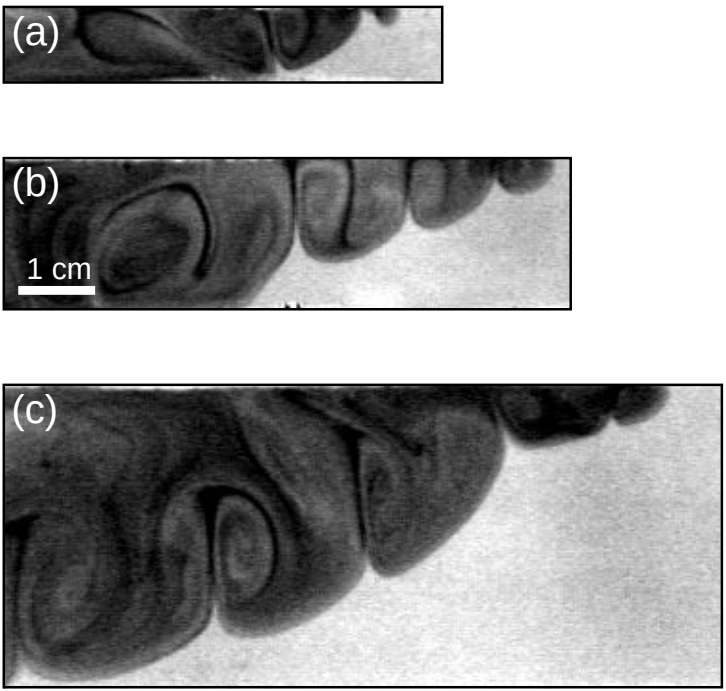
(a)
(b)
1 cm
(c)

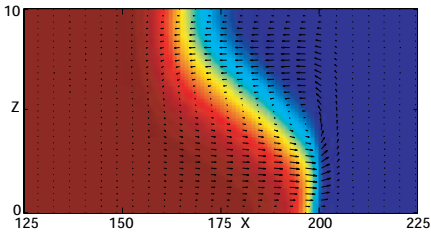
10
Z
0
125
150
175
X
200
225

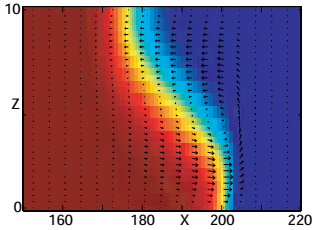
10
Z
0
160
180
X
200
220

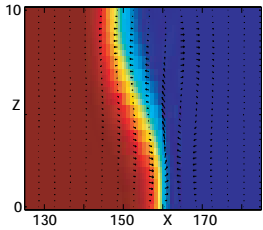
10
Z
0
130
150
X
170

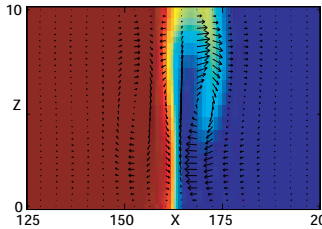
10
Z
0
125
150
X
175
200

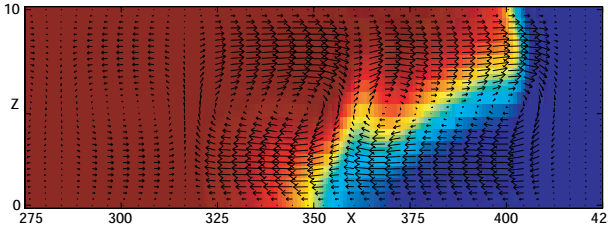
10
Z
0
275
300
325
350
X
375
400
425

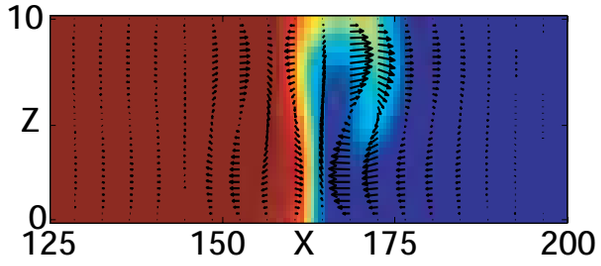
10
Z
0
125
150
X
175
200

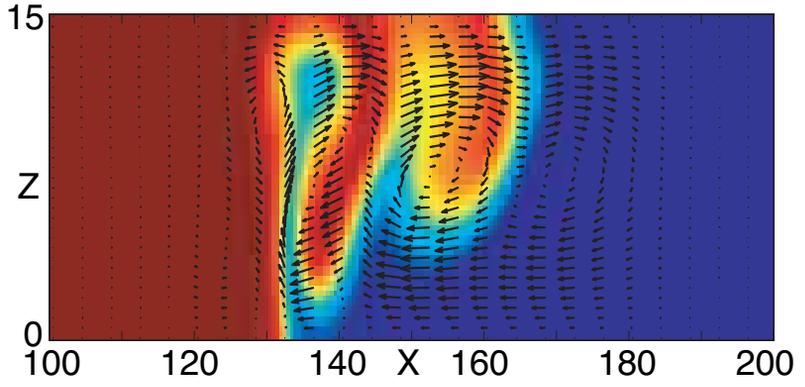
15
Z
0
100
120
140
X
160
180
200

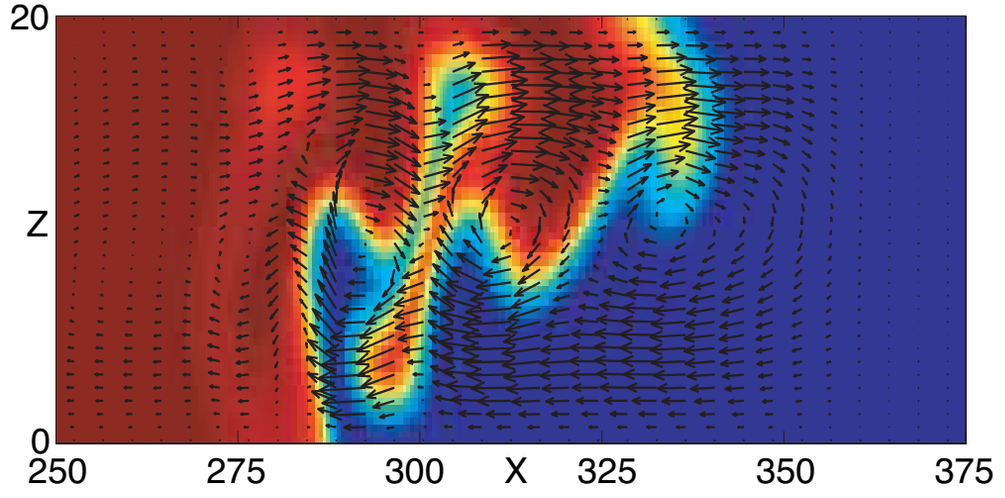
20
Z
0
250
275
300
X
325
350
375

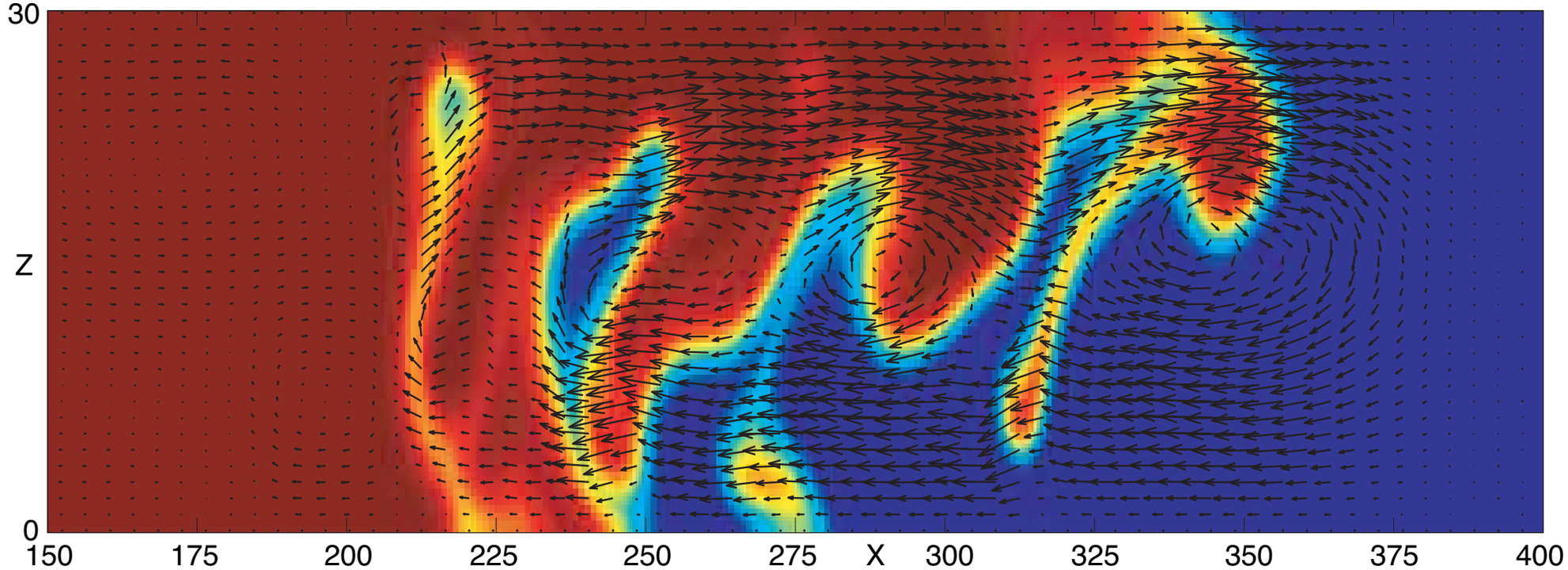
30
Z
0
150
175
200
225
250
275
X
300
325
350
375
400

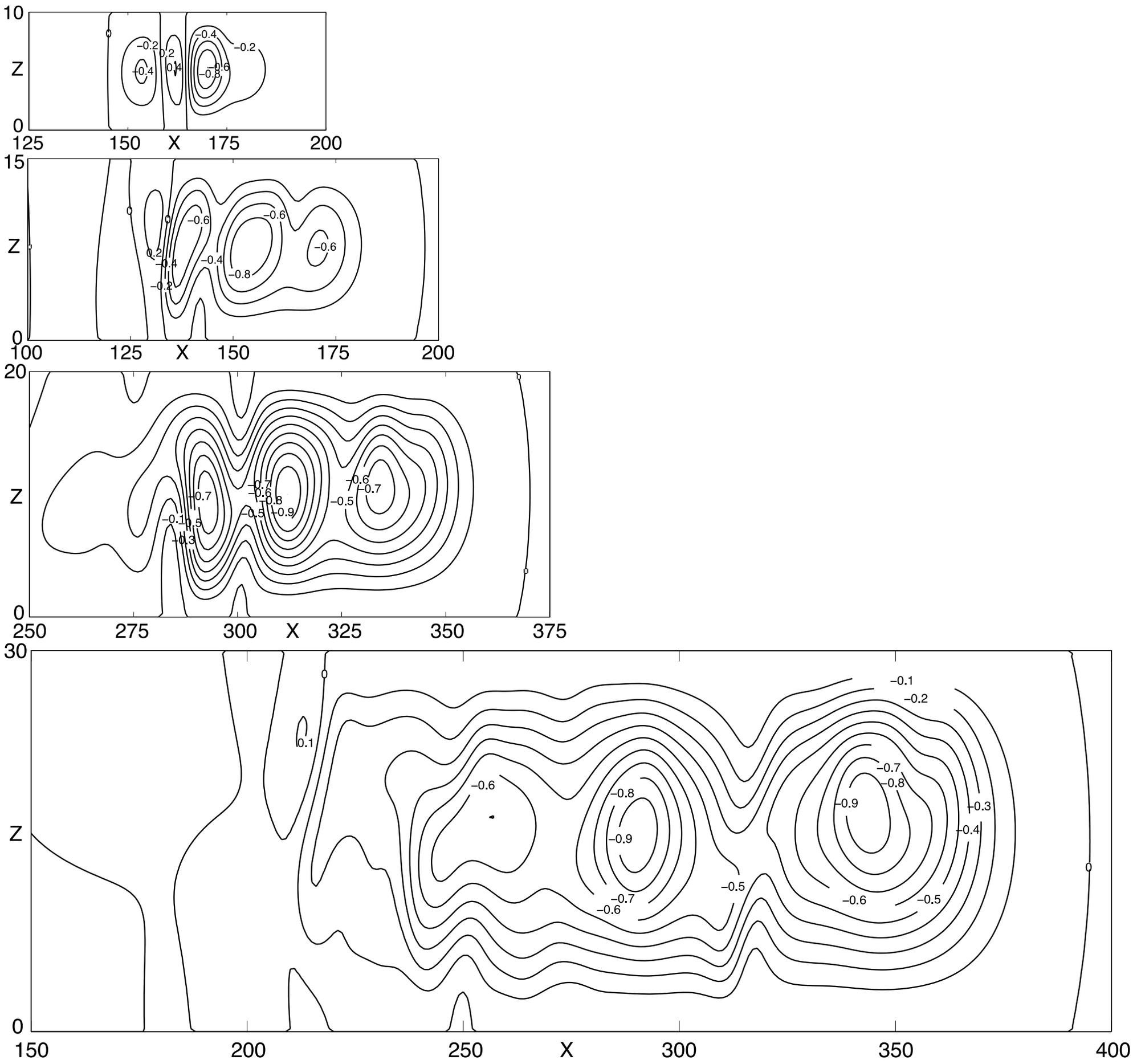
10
Z
0
125
150
X
175
200
15
Z
0
100
125
X
150
175
200
20
Z
0
250
275
300
X
325
350
375
30
Z
0
150
200
250
X
300
350
400